Chemical Physics 568 (2023) 111843

Contents lists available at ScienceDirect

Chemical Physics

journal homepage: www.elsevier.com/locate/chemphys

Characterization of competing halogen-bonding and hydrogen-bonding motifs in the acetonitrile/hydrogen iodide dimer

Morgan A. Perkins, Gregory S. Tschumper *

Department of Chemistry and Biochemistry, University of Mississippi, University, MS 38677–1848, USA

ARTICLE INFO

Keywords:
Halogen bonding
Hydrogen bonding
Harmonic vibrational frequencies
Complete basis set limit
CCSD(T)
Dissociation energy

ABSTRACT

Three different C_{3v} configurations of the CH_3CN/HI dimer have been characterized using MP2 and CCSD(T) methods with large correlation consistent basis sets. All three stationary points are minima. The hydrogen bonded $CH_3CN\cdots HI$ configuration is the global minimum (GM) with an electronic dissociation energy exceeding 4 kcal mol^{-1} near the CCSD(T) complete basis set (CBS) limit. A strongly bound halogen-bonded form of the dimer, $CH_3CN\cdots IH$, lies within 0.9 kcal mol^{-1} of the GM according to CCSD(T) electronic energies extrapolated to the CBS limit. The energetic separation between the two minima decreases by approximately 0.1 kcal mol^{-1} at all levels of theory when the harmonic zero-point vibrational energies are included. A third minimum was identified in which iodine interacts with the hydrogens of the methyl group ($HI\cdots CH_3CN$). This minimum is significantly higher in energy than the GM, almost within 1 kcal mol^{-1} of the dissociation limit. The GM has been previously identified via matrix isolation infrared spectroscopy. The energetics, vibrational frequencies, and infrared intensities computed here corroborate the tentative assignment of a second feature in the HI stretching region of the experimental infrared spectrum to the halogen-bonded configuration.

1. Introduction

Small dimers consisting of a base interacting with a hydrogen halide ($B\cdots HY$ where Y = F, Cl, Br, or I) have frequently been used as case studies for hydrogen bonding interactions [1–8]. Infrared (IR) spectroscopy and high-accuracy quantum computational chemistry are two tools that have been used to study fundamental aspects of hydrogen bonding in these systems. Vibrational frequency shifts, for example, can be used to identify the formation of weak non-covalent bonds such as hydrogen and halogen bonds. Quantum computational chemistry can be used in conjunction with gas-phase experimental work to aid the search for and assignment of spectral signatures. Direct comparison to experimental results obtained in a cryogenic matrix can be more challenging since matrices can have a stabilizing effect on hydrogen-bonded species, resulting in larger frequency shifts from the monomers, and can even distort the geometry of the complex compared to the gas-phase [9–11].

Acetonitrile (CH_3CN) is a moderately strong hydrogen bond acceptor. Hydrogen halides have been used as the hydrogen bond donor to CH_3CN in a number of experimental and computational studies, and the dissociation energies of these heterogeneous dimers have been found to range from roughly 80% to 180% of that for the paradigmatic water dimer [10–17]. Among the hydrogen halide species that can interact with CH_3CN by donating a hydrogen bond, HI is of particular interest because of its potential to also form an energetically competitive halogen-bonded species [18–20]. Such a complex would have the iodine atom of HI interacting with the acetonitrile nitrogen ($CH_3CN\cdots IH$). In the 1980s, a series of IR spectroscopy studies looked at the CH_3CN/HI dimer and associated monomers in low-temperature, solid matrices [14,21–24]. The initial focus of the earliest study was the characterization of the hydrogen-bonded CH_3CN/HI dimer. However, changing spectral features upon irradiating the hydrogen-bonded dimer revealed that a second, non-hydrogen-bonded form of the dimer existed. The studies that followed aimed to better characterize the relationship between these two different forms of the CH_3CN/HI dimer. A subsequent study by Barnes looked at CH_3CN/HI along with the N,N-dimethylacetamide (DMA)/HI dimer, which had also been found to exist in two different forms [25]. Barnes was the first to suggest several different possible configurations for the non-hydrogen-bonded form of these dimers and concluded that a "reverse" orientation ($CH_3CN\cdots IH$) was most likely to be the arrangement of the two dimers. Though these results have been briefly mentioned by a few more recent studies [9,11,26], to the best of our knowledge a more extensive investigation has not been undertaken. This study will perform the first systematic computational analysis of the various possible CH_3CN/HI

* Corresponding author.
E-mail address: tschumpr@olemiss.edu (G.S. Tschumper).

https://doi.org/10.1016/j.chemphys.2023.111843
Received 13 December 2022; Received in revised form 25 January 2023; Accepted 31 January 2023
Available online 2 February 2023

dimer configurations. Structural and energetic analyses will be performed for all identified stationary points. Additionally, harmonic vibrational frequency shifts and IR intensities will be computed. This data will facilitate the interpretation of available experimental spectra and also serve as a guide for future studies of this small dimer system where both halogen- and hydrogen-bonded configurations appear to be experimentally accessible.

2. Computational details

Three different configurations of the CH_3CN/HI dimer and the associated monomers were fully optimized using the MP2 [27] and CCSD(T) [28–30] methods along with a correlation consistent basis set series augmented with diffuse functions on all atoms except hydrogen and using a relativistic pseudopotential for the 28 core electrons of iodine atoms: cc-pVXZ for H, aug-cc-pVXZ for C and N, and aug-cc-pVXZ-PP for I, for $X = T$ and Q [31–37]. These basis sets are denoted heavy-aug-cc-pVXZ or ha$X$Z because only the heavy (non-hydrogen) atoms are augmented with diffuse functions. This reduces the total number of basis functions while still accurately describing hydrogen bonding, halogen bonding, and other non-covalent interactions [20,38–43].

Harmonic vibrational frequency computations were performed with the same series of methods and basis sets in order to confirm that each stationary point identified was a minimum on the potential energy surface. Single-point energy computations for the monomers and dimer minima were performed using MP2/ha5Z and CCSD(T)/ha5Z on each method's respective haQZ geometry. Relative electronic energies and dissociation energies near the complete basis set (CBS) limit were obtained from ha$X$Z single-point computations on the haQZ geometry using separate algebraic expressions to extrapolate the Hartree–Fock energy and correlation energy (Eqs. (1) and (2), respectively) [44–46]. The CBS-limit Hartree–Fock energy was obtained using the three-parameter exponential function proposed by Feller with the entire basis set series (X = T, Q, 5) [47]. Using the largest two basis sets (X = Q and 5), the CBS-limit electronic correlation energy was obtained using the two-parameter inverse-cubic function described by Helgaker and co-workers [48].

$$E_{HF}^{CBS} = E_{HF}^{5Z} - \frac{(E_{HF}^{5Z} - E_{HF}^{QZ})^2}{E_{HF}^{TZ} - 2E_{HF}^{QZ} + E_{HF}^{5Z}} \quad (1)$$

$$E_{c}^{CBS} = \frac{125E_{c}^{5Z} - 64E_{c}^{QZ}}{61} \quad (2)$$

All geometry optimizations were performed using analytic gradients. Analytic Hessians were used for all MP2 computations while numerical Hessians obtained from finite differences of analytic gradients were used for the CCSD(T) computations. The frozen-core approximation was used for all geometry optimizations and harmonic vibrational frequency computations. The two core electrons of C and N were excluded from the correlation procedure. For I, 28 core electrons were replaced with the 28 MDF pseudopotential, followed by 8 additional core electrons being excluded from the correlation procedure. All MP2 and CCSD(T) computations were performed using `Gaussian16` [49] and `CFOUR` [50], respectively.

Dissociation energies were computed for each system's global minimum. Computing electronic dissociation energies using finite basis sets gives rise to an inconsistency known as basis set superposition error (BSSE) [51,52]. In order to assess the effect of BSSE on the systems examined here, the counterpoise procedure (CP) [53–55] was employed, following the procedure outlined elsewhere [56].

Table 1
CCSD(T)/haQZ intramolecular bond lengths (in Å) and angles (in degrees) for the CH_3CN/HI dimer configurations and associated monomers.

	r(HI)	r(NC)	r(CC)	r(CH)	A(CCH)
HI	1.602	N/A	N/A	N/A	N/A
CH_3CN	N/A	1.159	1.464	1.089	109.77
HB	1.609	1.158	1.463	1.088	109.69
XB	1.607	1.158	1.463	1.089	109.73
LM	1.601	1.159	1.463	1.089	109.72

3. Results

3.1. Structures

Three different minima were identified for the CH_3CN/HI mixed dimer: the hydrogen-bonded global minimum (GM) where HI donates the hydrogen bond ($CH_3CN\cdots$HI, labeled HB), a halogen-bonded minimum ($CH_3CN\cdots$IH, labeled XB), and a second local minimum where the iodine is now pointing towards the methyl group (HI$\cdots CH_3CN$, labeled LM). The configurations are all highly symmetric, each one having C_{3v} symmetry. All three minima are depicted in Fig. 1. The HB configuration has been characterized in experimental work, and based on IR spectral signatures differing from that of HB, a second, non-hydrogen-bonded CH_3CN/HI configuration has been experimentally identified and postulated to have a halogen-bonded configuration [14,21–24]. The LM stationary point is identified for the first time in this work.

Table 1 presents the intramolecular bond lengths and CCH angle for the monomers CH_3CN and HI as well as all three dimer minima at the CCSD(T)/haQZ level of theory. The changes in the intramolecular bond lengths (Δr) are less than or equal to ±0.001 Å for all but the HI bond. The magnitude of Δr(HI) is nearly the same for HB and XB, +0.007 and +0.005 Å, respectively. The CCH angle in CH_3CN undergoes relatively minor changes upon dimerization. The angle decreases for all configurations, with the largest change being a decrease of 0.08° for HB. Key CCSD(T)/haQZ intermolecular bond lengths are presented in Fig. 1. HB has the largest distance between iodine and the nearest heavy atom on CH_3CN: r(N$\cdots$I) = 3.77 Å, though that includes the length of the HI covalent bond. The intermolecular hydrogen bond for HB is only 2.17 Å, whereas the intermolecular halogen bond length for XB is 3.18 Å, both at the CCSD(T)/haQZ level of theory. The analogous value for LM is 3.67 Å, similar to the value for HB.

An analogous table, including intermolecular bond length values, is provided in the Supplementary Material for MP2/haQZ results. Overall, MP2 produces similar geometric parameters to CCSD(T), with the intramolecular and intermolecular bond lengths differing by no more than 0.01 Å and 0.10 Å, respectively, and the angles by no more than 0.2 degrees. The MP2 and CCSD(T) Cartesian coordinates of the optimized monomers and dimer configurations for all basis sets are provided in the Supplementary Material.

3.2. Energetics

The MP2 and CCSD(T) relative electronic energies (ΔE) for all of the minima are tabulated in Table 2 and the values with harmonic zero-point vibrational energy (ZPVE) corrections are provided in Table 3. The dissociation energy of HB is also listed in both tables, with (D_0) and without (D_e) harmonic ZPVE corrections. The electronic dissociation energy of HB is approximately 4 kcal mol^{-1} near the CCSD(T) CBS limit, which is only slightly smaller than the corresponding value for the water dimer, *ca.* 5 kcal mol^{-1} [57]. Including harmonic ZPVE reduces the D_e by about 1 kcal mol^{-1} for both MP2 and CCSD(T). Regardless of the basis set used, MP2 overestimates both D_e and D_0 by approximately 0.8 kcal mol^{-1}. Results from using the CP procedure to obtain the dissociation energy (D_e^{CP}) can be found in the Supplementary Material. The D_e^{CP} values differ from D_e by no more than 0.6 kcal mol^{-1} (*ca.* 13%)

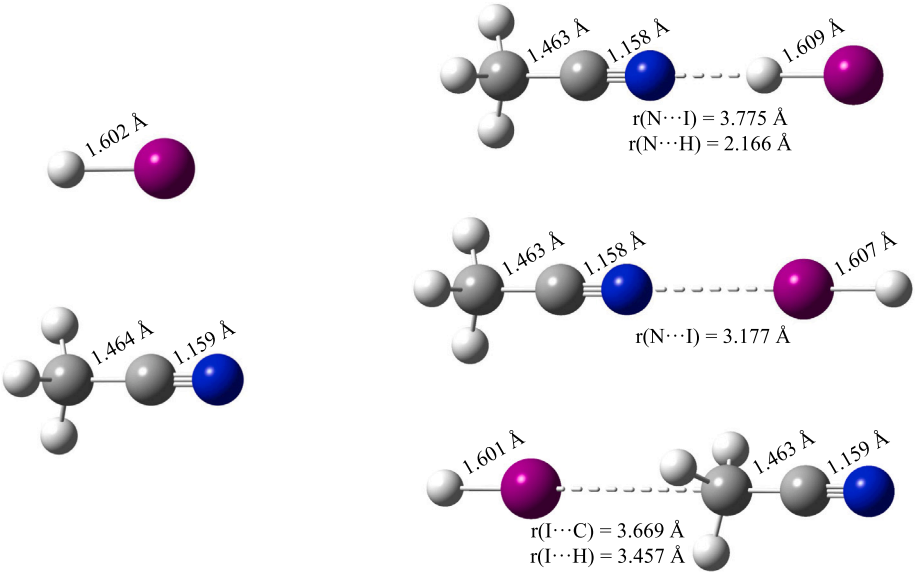

Fig. 1. The monomers (left) and three C_{3v} CH_3CN/HI dimer minima (right) characterized in this study, HB (top), XB (middle), and LM (bottom), with key CCSD(T)/haQZ intermolecular and intramolecular bond distances labeled.

Table 2
MP2 and CCSD(T) relative electronic energies in kcal mol^{-1} of the CH_3CN/HI dimer minima as well as the electronic dissociation energy for the global minimum (D_e).

	MP2				CCSD(T)			
	haTZ	haQZ	ha5Z[a]	CBS[a]	haTZ	haQZ	ha5Z[a]	CBS[a]
HB	0.00	0.00	0.00	0.00	0.00	0.00	0.00	0.00
XB	0.90	0.89	1.07	1.28	0.57	0.61	0.74	0.89
LM	3.55	3.50	3.50	3.53	3.01	2.97	2.97	2.98
D_e	4.93	4.99	4.95	4.93	4.17	4.19	4.13	4.09

[a]From single-point computations performed on the corresponding haQZ optimized structures.

Table 3
Harmonic ZPVE-corrected relative energies (ΔE_0) and dissociation energies (D_0) in kcal mol^{-1} of the CH_3CN/HI dimer minima using MP2 and CCSD(T) methods.

	MP2				CCSD(T)			
	haTZ	haQZ	ha5Z[a]	CBS[a]	haTZ	haQZ	ha5Z[a]	CBS[a]
HB	0.00	0.00	0.00	0.00	0.00	0.00	0.00	0.00
XB	0.80	0.79	0.97	1.18	0.46	0.53	0.66	0.81
LM	2.86	2.83	2.84	2.86	2.28	2.30	2.29	2.30
D_0	3.92	4.00	3.96	3.94	3.16	3.23	3.17	3.13

[a]Values calculated using the haQZ harmonic ZPVE corrections.

near the MP2 CBS limit and by no more than 0.4 kcal mol^{-1} (*ca.* 10%) near the CCSD(T) CBS limit.

The halogen-bonded minimum is relatively energetically competitive with GM, being only 0.9 kcal mol^{-1} higher in energy than HB at the CCSD(T) CBS limit. Comparatively, LM is significantly higher in energy, with a ΔE at or above 3 kcal mol^{-1} at both the MP2 and CCSD(T) levels of theory using all three basis sets. The ZPVE-corrected relative energies (Table 3) obtained from both MP2 and CCSD(T) harmonic frequencies consistently decrease ΔE by 0.1 kcal mol^{-1} for XB and 0.7 kcal mol^{-1} for LM. The decrease in the HI stretching frequency induced by hydrogen bonding in the HB minimum (vida infra) results in a positive contribution to the ZPVE correction for the relative energy of the XB structure. However, the net ZPVE correction for XB ends up being slightly negative (−0.1 kcal mol^{-1}), due to the contributions from a degenerate, intermolecular vibrational mode. This vibrational frequency associated with the off-axis bending (or wagging) of the H atom in hydrogen iodide increases appreciably in the HB structure, where HI donates a hydrogen bond to the *N* atom of acetonitrile. The energetics and harmonic vibrational frequencies computed in this investigation have also been used (without any scaling factors) to estimate the thermochemistry associated with the formation of these dimers near room temperature. Similar to the water dimer [58,59], formation of the low-energy HB and XB isomers is exergonic near 0K by approximately −3 kcal mol^{-1}. However, the free energies of association for $(H_2O)_2$, HB, and XB become more positive as the temperature increases, yielding endergonic formations ($\Delta G° > 0$) at 298 K.

3.3. Harmonic vibrational frequencies

The MP2 and CCSD(T) hydrogen iodide harmonic stretching frequencies (ω_{HI}) for the isolated HI monomer are presented in Table 4. Upon complexation, this stretching frequency undergoes a shift ($\Delta\omega_{HI}$) as a result of HI participating in a weak non-covalent interaction, such as a hydrogen or halogen bond. Our recent study of the similar HCN/HI dimer noted that the HI MP2/haQZ and CCSD(T)/haQZ stretching frequency was anomalously large compared to the haTZ and ha5Z results, though the frequency shifts remained relatively consistent [20]. This same trend is also observed in the current study.

The HI stretch has one of the most significant vibrational frequency changes from the HI and CH_3CN monomers to the dimer formations. The most significant shift occurs for the hydrogen-bonded configuration: −59 cm^{-1} at the CCSD(T)/haQZ level of theory. This shift is also associated with a significant increase in the IR intensity of the HI stretching mode, going from less than 0.1 km mol^{-1} for the monomer to over 200 km mol^{-1} when computed with the CCSD(T) method and haQZ basis set. The $\Delta\omega_{HI}$ value is less pronounced for XB at only −24 cm^{-1}, with an appreciable intensity of 15.8 km mol^{-1}. There is little to no shift in the HI stretching frequency for LM, and the IR intensity also does not change from the monomer. As can be seen from data provided in the Supplementary Material, one of the only significant vibrational frequency shifts for LM is the methyl group CH symmetric and antisymmetric stretches, though in comparison to $\Delta\omega_{HI}$ the values are small: −8 cm^{-1} and −7 cm^{-1} for the symmetric and antisymmetric stretch, respectively, at the CCSD(T)/haQZ level of theory. MP2 significantly overestimates $\Delta\omega_{HI}$ for HB by as much as 86 cm^{-1} and overestimates the equivalent values for XB and LM by only

Table 4
MP2 and CCSD(T) harmonic stretching frequencies (ω_{HI} in cm^{-1}) and IR intensities (I in km mol^{-1}) of the isolated HI monomer and the corresponding frequency shifts ($\Delta\omega_{HI}$) and IR intensities induced by the formation of a weak non-covalent interaction in the different CH_3CN/HI minima.

	HI		HB		XB		LM	
	ω_{HI}	I	$\Delta\omega_{HI}$	I	$\Delta\omega_{HI}$	I	$\Delta\omega_{HI}$	I
MP2/haTZ	2414	0.4	−121	487.3	−22	12.1	0	0.4
MP2/haQZ	2455	0.8	−135	538.1	−26	11.5	−2	0.9
CCSD(T)/haTZ	2338	0.1	−34	62.2	−20	17.1	+3	0.1
CCSD(T)/haQZ	2377	0.0	−59	203.0	−24	15.8	+1	0.0

2 to 3 cm^{-1}. For the methyl group CH shifts, MP2 results stay within 1 cm^{-1} of the CCSD(T) results. The MP2 and CCSD(T) vibrational frequencies and intensities for the monomers and all forms of the dimer are reported in the Supplementary Material.

Harmonic vibrational frequency shifts can provide guides to differentiate between various configurations of a complex in experiment. Several experimental studies have reported IR spectra of the CH_3CN/HI dimer and associated monomers in solid, low-temperature nitrogen and argon matrices [14,21–24]. These papers focus on two primary vibrations: the HI stretch and the CN stretch of CH_3CN. Experimental HI vibrational frequency shifts fall between the MP2/haQZ and CCSD(T)/haQZ $\Delta\omega_{HI}$ values. The corresponding shift for XB has not been reported. The experimental CN stretch shifts, reported for both HB and XB in an argon matrix, are remarkably similar to the MP2 and CCSD(T) values obtained with haQZ. The CN shifts are very small, not exceeding +10 cm^{-1} according to the previously reported experimental results and computational results calculated from data provided in the Supplementary Material.

4. Conclusions

Three different C_{3v} configurations of the CH_3CN/HI dimer as well as their corresponding monomers have been examined using large correlation consistent basis sets with the MP2 and CCSD(T) methods. Two previously identified structures were examined: the global minimum hydrogen-bonded isomer ($CH_3CN\cdots HI$) and a local minimum halogen-bonded configuration ($CH_3CN\cdots IH$). A newly identified higher-energy minimum has also been characterized, which has the iodine atom oriented towards the H atoms of the methyl group of acetonitrile ($HI\cdots CH_3CN$). This configuration is only bound by *ca.* 1 kcal mol^{-1} and lies approximately 3 kcal mol^{-1} above the hydrogen bonded global minimum near the CCSD(T) CBS limit.

The global minimum has been identified in low-temperature matrix isolation studies using IR spectroscopy, and the vibrational frequency shifts used to characterize its formation are relatively close to the harmonic vibrational frequency results obtained in this study. For the HI vibrational frequency, the experimental shift in an argon matrix is −88 cm^{-1} and the CCSD(T)/haQZ value is −59 cm^{-1}. As noted in some previous studies, hydrogen-bonded species are typically stabilized in a matrix, which results in an increase in vibrational frequency shifts from the monomer species compared to gas-phase data. The CN experimental stretching frequency shift for the global minimum (+5 cm^{-1}) matches qualitatively to the computed values of +8 cm^{-1} and +3 cm^{-1} from MP2/haQZ and CCSD(T)/haQZ computations, respectively.

A second form of the dimer identified via IR spectroscopy has been proposed to have a halogen bonded structure ($CH_3CN\cdots IH$). While the exact value of the HI stretching frequency for that configuration has not been reported, researchers have noted that it is in the monomer stretching region. Additionally, small, positive CN experimental shifts akin to those seen in the hydrogen bonded configuration have also been reported for the potentially halogen-bonded form of the dimer. Computational results show that this configuration is energetically accessible, being approximately 0.8 kcal mol^{-1} higher in energy than the global minimum near the CCSD(T) CBS limit after including the harmonic zero-point vibrational energy. Computed harmonic shifts for $CH_3CN\cdots IH$ of −24 cm^{-1} (HI shift) and +8 cm^{-1} (CN shift) at the CCSD(T)/haQZ level of theory are consistent with experimental results, and provide further evidence connecting the additional infrared spectroscopic features to a second, halogen-bonded form of the CH_3CN/HI dimer.

The harmonic vibrational frequency data presented here have helped confirm the assignment of IR spectral features from matrix isolation experiments to two energetically competitive hydrogen-bonded and halogen-bonded minima of the CH_3CN/HI dimer. Theoretical fundamental vibrational frequencies would likely be a useful extension of this work, particularly for subsequent gas-phase experimental studies of this system that exhibit competition between hydrogen and halogen bonding. We plan to do an anharmonic analysis on both configurations after performing additional testing and calibration in order to resolve technical issues associated with second-order vibrational perturbation theory (VPT2) computations on these systems. That analysis will also provide more detailed insight into the spectroscopic perturbations induced by an inert matrix environment.

CRediT authorship contribution statement

Morgan A. Perkins: Conceptualization (equal), Formal analysis (lead), Investigation (lead), Visualization (lead), Writing – original draft (lead), Writing – review and editing (equal). **Gregory S. Tschumper:** Conceptualization (equal), Funding acquisition (lead), Supervision (lead), Writing – review and editing (equal).

Declaration of competing interest

The authors declare that they have no known competing financial interests or personal relationships that could have appeared to influence the work reported in this paper.

Data availability

The data that supports the findings of this study are available within the article and its Supplementary Material.

Acknowledgments

This work was supported in part by the National Science Foundation, United States (CHE-2154403).

Appendix A. Supplementary data

Supplementary material related to this article can be found online at https://doi.org/10.1016/j.chemphys.2023.111843. (additional energetic and structural data; harmonic vibrational frequencies and IR intensities; Cartesian coordinates)

References

[1] A.C. Legon, D.J. Millen, Determination of properties of hydrogen-bonded dimers by rotational spectroscopy and a classfication of dimer geometries, Faraday Discuss. Chem. Soc. 73 (1982) 71–87.
[2] A.J. Barnes, Molecular complexes of the hydrogen halides studied by matrix isolation infrared spectroscopy, J. Mol. Struct. 100 (1983) 259–280.
[3] A.C. Legon, D.J. Millen, Hydrogen bonding as a probe of electron densities: limiting gas-phase nucleophilicities and electrophilicities of B and HX, J. Am. Chem. Soc. 109 (1987) 356–358.
[4] Marshall T. Carroll, Richard F.W. Bader, An analysis of the hydrogen bond in BASE-HF complexes using the theory of atoms in molecules, Mol. Phys. 65 (1988) 695–722.
[5] P.A. Block, R.E. Miller, Near infrared spectroscopy of the HCN-HX (X = Cl, Br, and I) binary complexes, J. Mol. Spectrosc. 147 (1991) 359–369.

[6] K.G. Tokhadze, N.A. Tkhorzhevskaya, Infrared spectra of weak hydrogen-bonded complexes in cryogenic solutions, J. Mol. Struct. 270 (1992) 351–368.

[7] P.W. Fowler, A.C. Legon, S.A. Peebles, Rotational spectrum of HCN···HI and a comparison of properties in the series HCN···HX (X=F, Cl, Br, I and CN), Chem. Phys. Lett. 226 (1994) 501–508.

[8] Defang Duan, Fubo Tian, Zhi He, Xing Meng, Liancheng Wang, Changbo Chen, Xiusong Zhao, Bingbing Liu, Tian Cui, Hydrogen bond symmetrization and superconducting phase of HBr and HCl under high pressure: An ab initio study, J. Chem. Phys. 133 (2010) 074509.

[9] Austin J. Barnes, Zofia Mielke, Matrix effects on hydrogen-bonded complexes trapped in low-temperature matrices, J. Mol. Struct. 1023 (2012) 216–221.

[10] Nicole M. Weiss, Anna W. Waller, James A. Phillips, Infrared spectrum of CH_3CN-HCl in solid neon, and modeling matrix effects in CH_3CN-HCl and H_3N-HCl, J. Mol. Struct. 1105 (2016) 341–349.

[11] Austin J. Barnes, Matrix isolation studies of hydrogen bonding - an historical perspective, J. Mol. Struct. 1163 (2018) 77–85.

[12] Alan Hinchliffe, Hydrogen bonding in HCN···HF, HCN···HCl, CH_3CN···HF and CH_3CN···HCl; an ab initio SCF-MO study, Adv. Mol. Relax. Int. Pr. 19 (1981) 227–237.

[13] Janet E. Del Bene, Hydrogen bonding: Methodology and applications to complexes of HF and HCl with HCN and CH_3CN, Int. J. Quantum Chem. 44 (1992) 527–541.

[14] Louise Schriver, André Schriver, Jean-Pierre Perchard, Infrared matrix-isolation study of the molecular complexes between acetonitrile and hydrogen halides. evidence for reactivity differences within the halide series, J. Chem. Soc. Faraday Trans. II 81 (1985) 1407–1425.

[15] William O. George, Bryan F. Jones, Rhobert Lewis, Jason M. Price, Computations of medium strength hydrogen bonds-complexes of mono- and bi-functional carbonyl and nitrile compounds with hydrogen chloride, Phys. Chem. Chem. Phys. 2 (2000) 4910–4917.

[16] Nicolai Bork, Lin Du, Heidi Reiman, Theo Kurtén, Henrik G. Kjaergaard, Benchmarking ab initio binding energies of hydrogen-bonded molecular clusters based on FTIR spectroscopy, J. Phys. Chem. A 118 (2014) 5316–5322.

[17] Nicolai Bork, Ville Loukonen, Henrik G. Kjaergaar, Hanna Vehkamäki, Resolving the anomalous infrared spectrum of the MeCN-HCl molecular cluster using ab initio molecular dynamics, Phys. Chem. Chem. Phys. 16 (2014) 24685–24690.

[18] Lindsey N. Anderson, Fredy W. Aquino, Alexandra E. Raeber, Xi Chen, Bryan M. Wong, Halogen bonding interactions: Revised benchmarks and a new assessment of exchange vs dispersion, J. Chem. Theory Comput. 14 (2018) 180–190.

[19] Miroslav Medved', Alex Iglesias-Reguant, Heribert Reis, Robert W. Góra, Josep M. Luis, Robert Zaleśny, Partitioning of interaction-induced nonlinear optical properties of molecular complexes. II. Halogen-bonded systems, Phys. Chem. Chem. Phys. 22 (2020) 4225–4234.

[20] Morgan A. Perkins, Gregory S. Tschumper, Characterization of competing halogen- and hydrogen-bonding motifs in simple mixed dimers of HCN and HX (X = F, Cl, Br, and I), J. Phys. Chem. A 126 (2022) 3688–3695.

[21] Louise Schriver, André Schriver, Jean-Pierre Perchard, Infrared photodissociation of the CH3CN:HI hydrogen bonded 1:1 complex trapped in a nitrogen matrix, J. Chem. Phys. 84 (1986) 5553–5560.

[22] Anders Engdahl, Bengt Nelander, Hydrogen iodide in argon matrixes, J. Phys. Chem. 90 (1986) 6118–6121.

[23] Louise Schriver, André Schriver, Serge Racine, Jean-Pierre Perchard, Infrared study of the interconversion between two forms of the CH3CN:HI complex trapped in solid argon, Chem. Phys. 119 (1988) 95–106.

[24] A.J. Barnes, Infrared photochemistry of hydrogen-bonded complexes trapped in low-temperature matrices, J. Mol. Struct. 177 (1988) 209–220.

[25] Zofia Mielke, Austin J. Barnes, Infrared matrix isolation studies of complexes between N, N-dimethylacetamide and hydrogen halides. part 2.-Hydrogen iodide complexes, J. Chem. Soc. Faraday Trans. II 82 (1986) 447–455.

[26] Payam Kalhor, Jing Xu, Hamad Ashraf, Bobo Cao, Zhi-Wu Yu, Structural properties and hydrogen-bonding interactions in binary mixtures containing a deep-eutectic solvent and acetonitrile, J. Phys. Chem. B 124 (2020) 1229–1239.

[27] Christian Møller, Milton S. Plesset, Note on an approximation treatment for many electron systems, Phys. Rev. 46 (1934) 618.

[28] Jiří Čížek, On the correlation problem in atomic and molecular systems. calculation of wavefunction components in Ursell-type expansion using quantum-field theoretical methods, J. Chem. Phys. 45 (11) (1966) 4256–4266.

[29] G.D. Purvis, R.J. Bartlett, A full coupled-cluster singles and doubles model: The inclusion of disconnected triples, J. Chem. Phys. 76 (4) (1982) 1910.

[30] Krishnan Raghavachari, Gary W. Trucks, John A. Pople, Martin Head-Gordon, A fifth-order perturbation comparison of electron correlation, Chem. Phys. Lett. 157 (6) (1989) 479–483.

[31] Thom H. Dunning, Gaussian basis sets for use in correlated molecular calculations. I. The atoms boron through neon and hydrogen, J. Chem. Phys. 90 (1989) 1007–1023.

[32] Rick A. Kendall, Thom H. Dunning, Robert J. Harrison, Electron affinities of the first-row atoms revisited. systematic basis sets and wave function, J. Chem. Phys. 96 (1992) 6796–6806.

[33] David E. Woon, Thom H. Dunning, Gaussian basis sets for use in correlated molecular calculations. III. The atoms aluminum through argon, J. Chem. Phys. 98 (1993) 1358–1371.

[34] Kirk A. Peterson, David E. Woon, Thom H. Dunning, Benchmark calculations with correlated molecular wave functions. IV. The classical barrier height of the H+ H_2 →H_2+H reaction, J. Chem. Phys. 100 (1994) 7410–7415.

[35] Angela K. Wilson, David E. Woon, Kirk A. Peterson, Thom H. Dunning, Gaussian basis sets for use in correlated molecular calculations. IX. The atoms gallium through krypton, J. Chem. Phys. 110 (1999) 7667–7676.

[36] Kirk A. Peterson, Detlev Figgen, Erich Goll, Hermann Stoll, Michael Dolg, Systematically convergent basis sets with relativistic pseudopotentials. II. Small-core pseudopotentials and correlation consistent basis sets for the post-d group 16–18 elements, J. Chem. Phys. 119 (2003) 11113–11123.

[37] Kirk A. Peterson, Benjamin C. Shepler, Detlev Figgen, Hermann Stoll, On the spectroscopic and thermochemical properties of ClO, BrO, IO, and their anions, J. Phys. Chem. A 110 (2006) 13877–13883.

[38] Janet E. Del Bene, Ab initio molecular orbital study of the structures and energies of neutral and charged bimolecular complexes of water with the hydrides AHn (A = nitrogen, oxygen, fluorine, phosphorus, sulfur, and chlorine), J. Phys. Chem. 92 (1988) 2874–2880.

[39] Gregory S. Tschumper, Reliable Electronic Structure Computations for Weak Noncovalent Interactions in Clusters, John Wiley & Sons, Ltd, 2008, pp. 39–90, chapter 2.

[40] Adel M. ElSohly, Gregory S. Tschumper, Comparison of polarization consistent and correlation consistent basis sets for noncovalent interactions, Int. J. Quantum Chem. 109 (2009) 91–96.

[41] Ewa Papajak, Jingjing Zheng, Xuefei Xu, Hannah R. Leverentz, Donald G. Truhlar, Perspectives on basis sets beautiful: Seasonal plantings of diffuse basis functions, J. Chem. Theory Comput. 7 (2011) 3027–3034.

[42] Ibon Alkorta, Goar Sanchez-Sanz, José Elguero, Janet E. Del Bene, FCl:PCX complexes: Old and new types of halogen bonds, J. Phys. Chem. A 116 (2012) 2300–2308.

[43] Janet E. Del Bene, Ibon Alkorta, José Elguero, Anionic complexes of F- and Cl- with substituted methanes: Hydrogen, halogen, and tetrel bonds, Chem. Phys. Lett. 655–656 (2016) 115–119.

[44] Emily J. Carrell, C.M. Thorne, Gregory S. Tschumper, Basis set dependence of higher-order correlation effects in π-type interactions, J. Chem. Phys. 136 (1) (2012) 014103.

[45] Emily J. Carrell, C.M. Thorne, Gregory S. Tschumper, Erratum: Basis set dependence of higher-order correlation effects in π-type interactions [J. Chem. Phys. 136, 014103 (2012)], J. Chem. Phys. 153 (6) (2020) 069901.

[46] Morgan A. Perkins, Kayleigh R. Barlow, Katelyn M. Dreux, Gregory S. Tschumper, Anchoring the hydrogen sulfide dimer potential energy surface to juxtapose $(H_2S)_2$ with $(H_2O)_2$, J. Chem. Phys. 152 (21) (2020) 214306.

[47] David Feller, The use of systematic sequences of wave functions for estimating the complete basis set, full configuration interaction limit in water, J. Chem. Phys. 98 (9) (1993) 7059–7071.

[48] Trygve Helgaker, Wim Klopper, Henrik Koch, Jozef Noga, Basis-set convergence of correlated calculations on water, J. Chem. Phys. 106 (23) (1997) 9639–9646.

[49] M.J. Frisch, G.W. Trucks, H.B. Schlegel, G.E. Scuseria, M.A. Robb, J.R. Cheeseman, G. Scalmani, V. Barone, G.A. Peterson, H. Nakatsuji, X. Li, M. Caricato, A.V. Marenich, J. Bloino, B.G. Janesko, R. Gomperts, B. Mennucci, H.P. Hratchian, J.V. Ortiz, A.F. Izmaylov, J.L. Sonnenberg, D. Williams-Young, F. Ding, F. Lipparini, F. Egidi, J. Goings, B. Peng, A. Petrone, T. Henderson, D. Ranasinghe, V.G. Zakrzewski, J. Gao, N. Rega, G. Zheng, W. Liang, M. Hada, M. Ehara, K. Toyota, R. Fukuda, J. Hasegawa, M. Ishida, T. Nakajima, Y. Honda, O. Kitao, H. Nakai, T. Vreven, K. Throssell, J.A. Montgomery Jr., J.E. Peralta, F. Ogliaro, M.J. Bearpark, J.J. Heyd, E.N. Brothers, K.N. Kudin, V.N. Staroverov, T.A. Keith, R. Kobayashi, J. Normand, K. Raghavachari, A.P. Rendell, J.C. Burant, S.S. Iyengar, J. Tomasi, M. Cossi, J.M. Millam, M. Klene, C. Adamo, R. Cammi, J.W. Ochterski, R.L. Martin, K. Morokuma, O. Farkas, J.B. Foresman, D.J. Fox, Gaussian16 Revision C.01, Gaussian Inc., Wallingford CT, 2016.

[50] J.F. Stanton, J. Gauss, L. Cheng, M.E. Harding, D.A. Matthews, P.G. Szalay, CFOUR, Coupled-Cluster techniques for Computational Chemistry, a quantum-chemical program package. with contributions from A.A. Auer and R.J. Bartlett and U. Benedikt and C. Berger and D.E. Bernholdt and Y.J. Bomble and L. Cheng and O. Christiansen and M. Heckert and O. Heun and C. Huber and T.-C. Jagau and D. Jonsson and J. Jusélius and K. Klein and W.J. Lauderdale and D.A. Matthews and T. Metzroth and L.A. Mück and D.P. O'Neill and D.R. Price and E. Prochnow and K. Ruud and F. Schiffmann and W. Schwalbach and S. Stopkowicz and A. Tajti and J. Vázquez and F. Wang and J.D. Watts and the integral packages MOLECULE (J. Almlöf and P.R. Taylor) and PROPS (P.R. Taylor) and ABACUS (T. Helgaker and H.J. Aa. Jensen and P. Jørgensen and

J. Olsen) and ECP routines by A. V. Mitin and C. van Wüllen. For the current version see http://www.cfour.de.

[51] Neil R. Kestner, He-He interaction in the SCF-MO approximation, J. Chem. Phys. 48 (1968) 252–257.

[52] B. Liu, A.D. McLean, Accurate calculation of the attractive interaction of two ground state helium atoms, J. Chem. Phys. 59 (1973) 4557–4558.

[53] H.B. Jansen, P. Ros, Non-empirical molecular orbital calculations on the protonation of carbon monoxide, Chem. Phys. Lett. 3 (1969) 140–143.

[54] S.F. Boys, F. Bernardi, The calculation of small molecular interactions by the differences of separate total energies. some procedures with reduced errors, Mol. Phys. 19 (1970) 553–566.

[55] Sílvia Simon, Miquel Duran, J.J. Dannenberg, How does basis set superposition error change the potential surfaces for hydrogen-bonded dimers? J. Chem. Phys. 105 (1996) 11024–11031.

[56] Gregory S. Tschumper, Reliable electronic structure computations for weak non-covalent interactions in clusters, Rev. Comput. Chem. 26 (2009) 39–90.

[57] Gregory S. Tschumper, Matthew L. Leininger, Brian C. Hoffman, Edward F. Valeev, Henry F. Schaefer, Martin Quack, Anchoring the water dimer potential energy surface with explicitly correlated computations and focal point analyses, J. Chem. Phys. 116 (2002) 690–701.

[58] L.A. Curtiss, D.J. Frurip, M. Blander, Studies of molecular association in H_2O and D_2O vapors by measurement of thermal conductivity, J. Chem. Phys. 71 (1979) 2703–2711.

[59] Meghan E. Dunn, Emma K. Pokon, George C. Shields, Thermodynamics of forming water clusters at various temperatures and pressures by Gaussian-2, Gaussian-3, Complete Basis Set-QB3, and Complete Basis Set-APNO Model Chemistries; implications for atmospheric chemistry, J. Am. Chem. Soc. 126 (2004) 2647–2653.